Supplementary file

Nanoscale magnetic imaging enabled by nitrogen vacancy centres in nanodiamonds labelled by iron-oxide nanoparticles

Martina Barbiero[1,2], Stefania Castelletto[3], Qiming Zhang[8], Ye Che[4], Mirren Charnley[4,5], Sarah Russell[4,6,7] and Min Gu[1,8,*]

[1]Laboratory of Artificial-Intelligence Nanophotonics, School of Science, RMIT University, Melbourne, Victoria 3001, Australia; [2]Division of Cancer Biology, The Institute of Cancer Research, London, United Kingdom; [3]School of Engineering, RMIT University, Melbourne, Victoria 3000, Australia; [4]Centre for Micro-Photonics, Faculty of Science, Engineering and Technology, Swinburne University of Technology, PO Box 218, Hawthorn, Victoria 3122, Australia; Immune Signalling Laboratory, Peter MacCallum Cancer Centre, Parkville, VIC, Australia; [5]Biointerface Engineering Group, Faculty of Science, Engineering and Technology, Swinburne University of Technology, Hawthorn, VIC, Australia; [6]Department of Pathology, The University of Melbourne, Parkville, VIC, Australia; [7]Sir Peter MacCallum Department of Oncology, The University of Melbourne, Parkville, VIC, Australia; [8]Centre for Artificial-Intelligence Nanophotonics, School of Optical-Electrical and Computer Engineering, University of Shanghai for Science and Technology, Shanghai, 200093, China.

[*]Correspondence: Min Gu, Email: gumin@usst.edu.cn

Description: Supplementary Figures and References

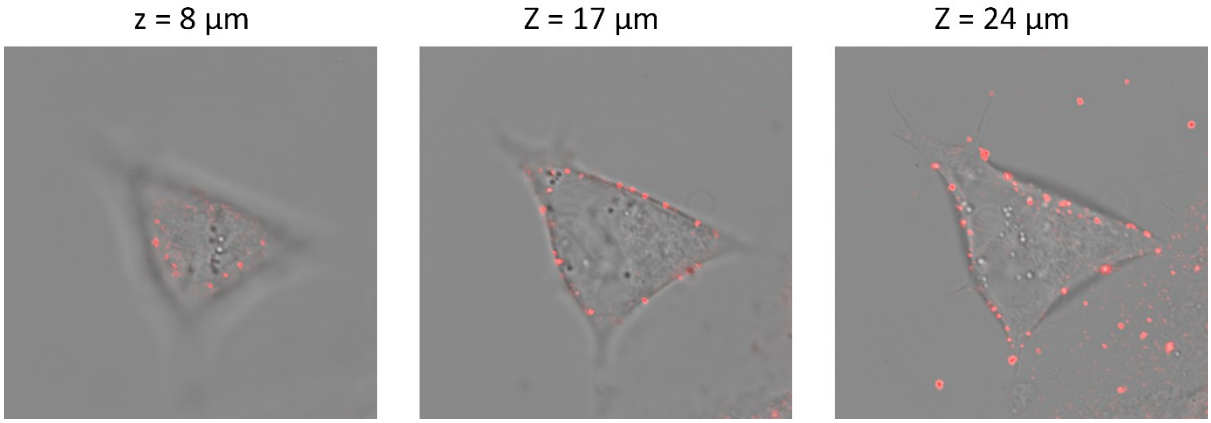

Fig. S1 | Co-localisation imaging of cells and NDs. Widefield images at three different focal plans ($z = 8\ \mu m; z = 17\ \mu m; z = 24\ \mu m$) with a 561 nm laser beam and a LED source. The images are taken to co-localise NDs labelling the cells.

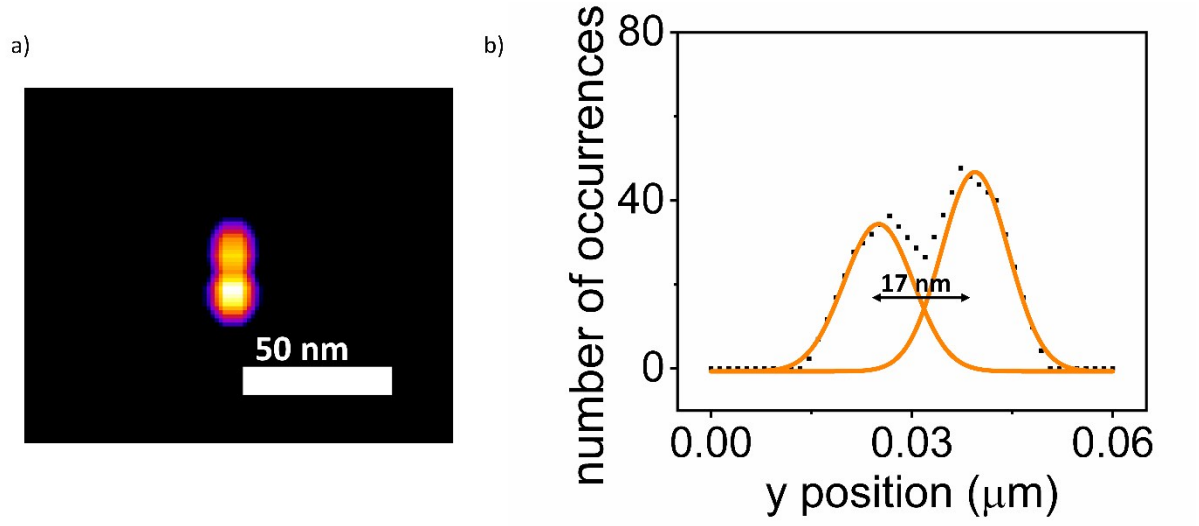

Fig. S2 | Superresolution of nitrogen vacancy (NV^-) centres. *(c)* Superresolved image of NV centres. *(b)* The reconstructed image has a full width at half maximum (FWHM) of 17 nm in the *y*-direction.

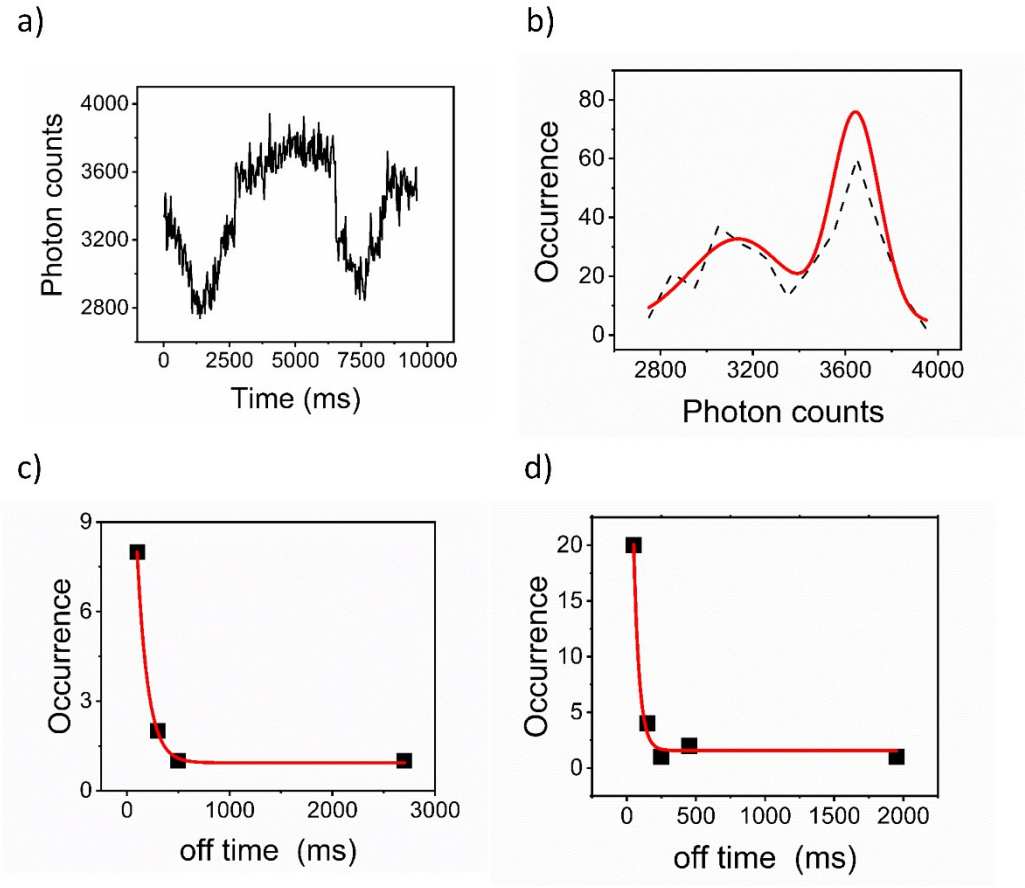

Fig. S3 | Blinking fluorescence study. *(a)* Blinking fluorescence recorded for a ND, the exposure time is 30 ms. *(b)* The photon counts per occurrence has two distribution states. *(c)* The 'on' time duration calculated from the fluorescence intensities which represent the 'on' state of the blinking emission. An exponential decay fitting is performed. The on time probability distribution shows a $\tau_{ON} = 73\ ms$. *(d)* The 'off' time duration calculated from the fluorescence intensities which represent the 'off' state of the blinking emission. An exponential decay fitting is performed. The off time probability distribution shows a $\tau_{OFF} = 27\ ms$

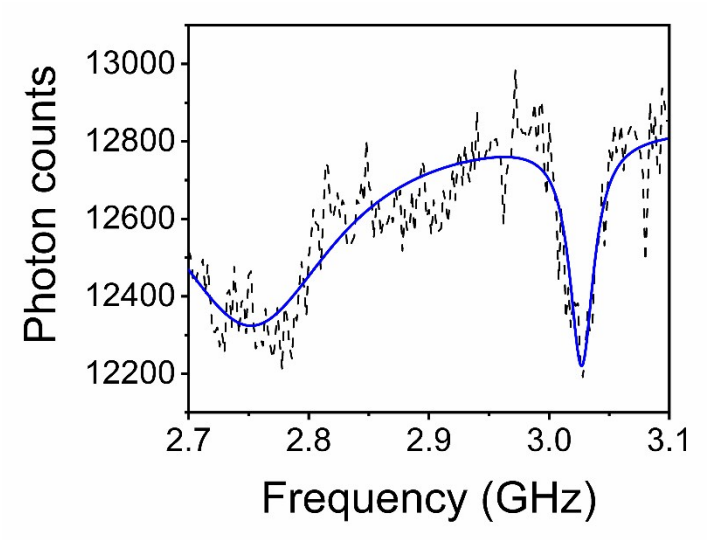

Fig. S4| ODMR signal for a biotinylated ND without use of MNPs. Two lorentian dips away from the Zeeman frequency can be measured at 2.75 GHz and 3.02 GHz respectively.

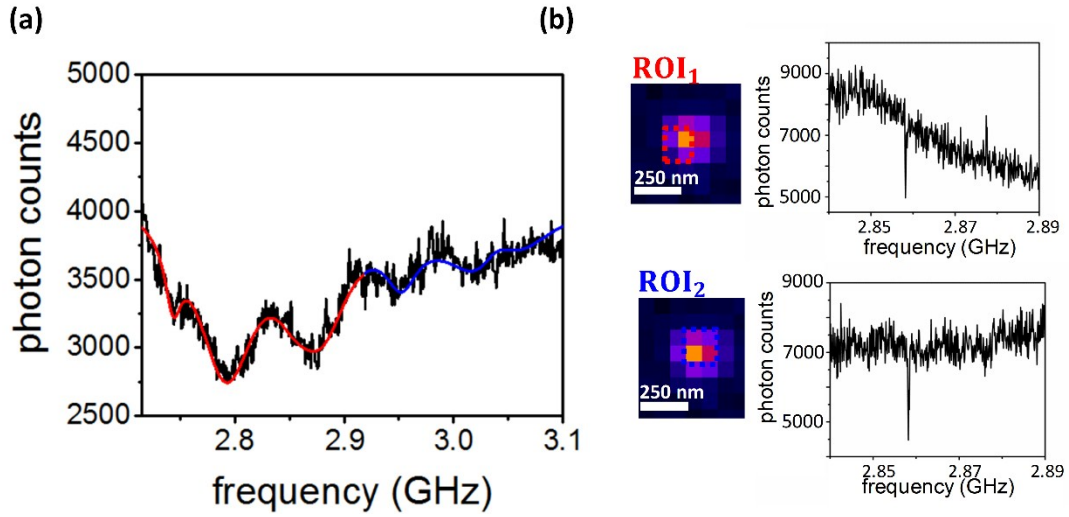

Fig. S5 | Nanoscale magnetic resonance. *(a)* ODMR for a selected ND. The signal is measured after an external magnetic field has magnetised the MNPs and then removed. *(b)* The fluorescence trace in RO^{I}_{1} shows a decrease at the ODMR frequency. In RO^{I}_{2} the fluorescence trace does not show any decrease at the ODMR frequency.

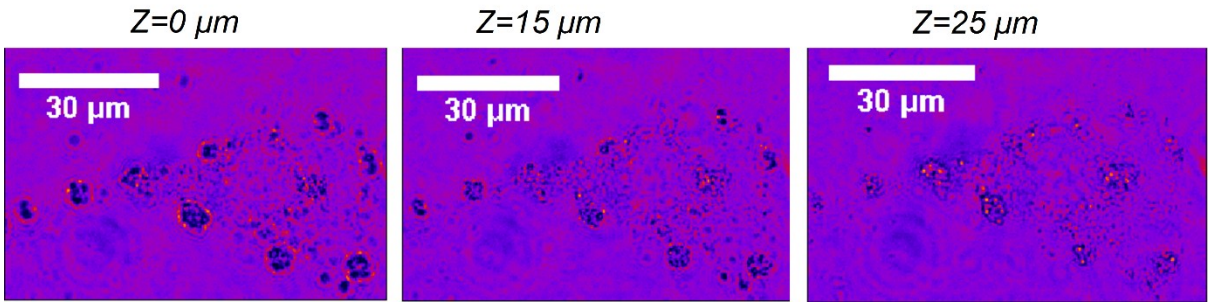

Fig. S6 | Cellular thickness. Z-stack of a MCF10A cell labelled with MNPs and NDs. The images are acquired with a widefield microscope and a bright field illumination. The cellular thickness is calculated from the *z*-stack performed on 50 MCF10A cells. We calculate an average cellular thickness is of $z = 25\ \mu m$. Furthermore, NDs labelling the cell are located on the cellular surface at $z = 25\ \mu m$.

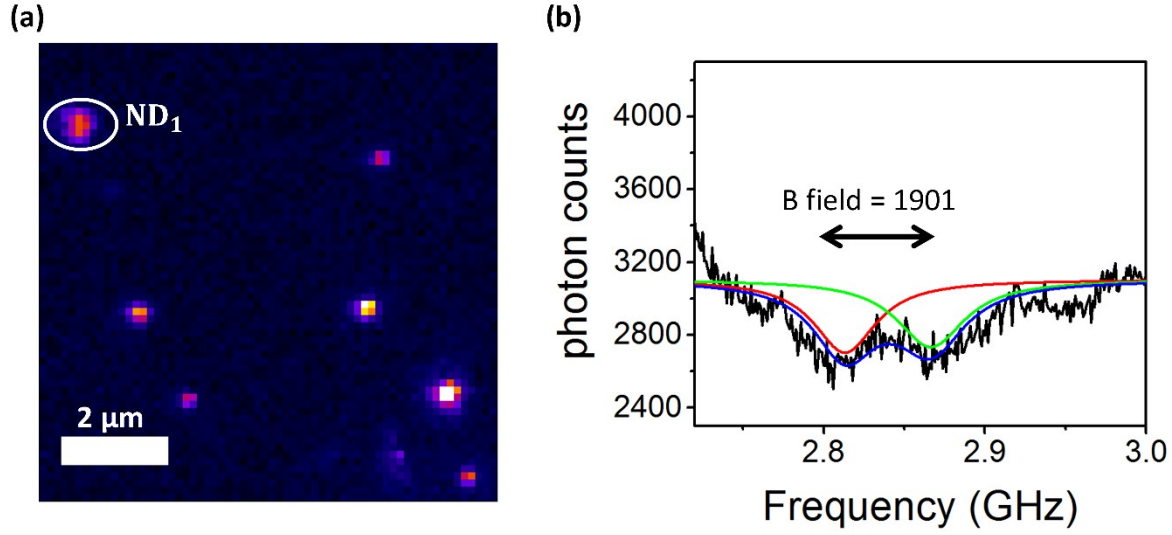

Fig. S7 | A ND is selected to calculate the magnetic field distribution. *(a)* Widefield image of NDs labelling a MCF10A cell. ND_1 is selected to measure the magnetic field via ODMR signal. *(b)* ODMR signal showing that ND_1 is sensing a magnetic field of 1901 μT.

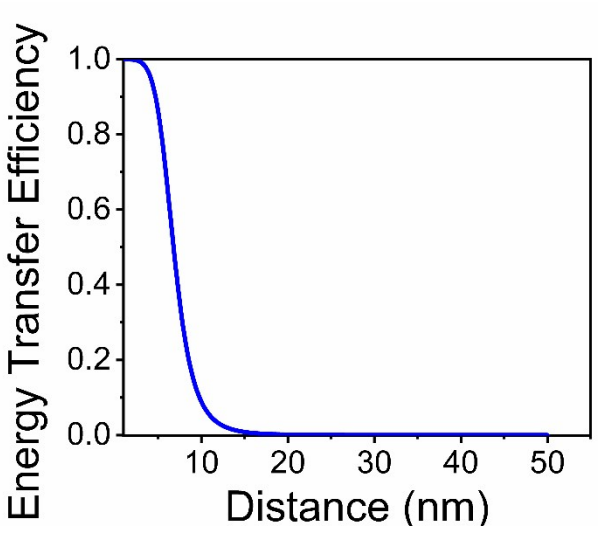

Fig. S8 | Simulated Energy transfer efficiency as a function of MNP-ND distance. NDs are labelled with MNPs via biotin- streptavidin. Only the NV centres on the ND surface contribute to the energy transfer between ND and MNPs.[1]

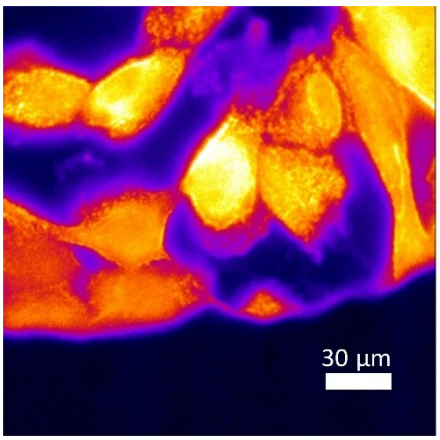

Fig. S9 | Cells labelled with streptavidin coated MNPs and Atto 555-biotin dye. Widefield image of MCF10A cells labelled with streptavidin coated MNPs. The MNPs are bounded to Atto 555-biotin dye. The MNPs uniformely label the cells.

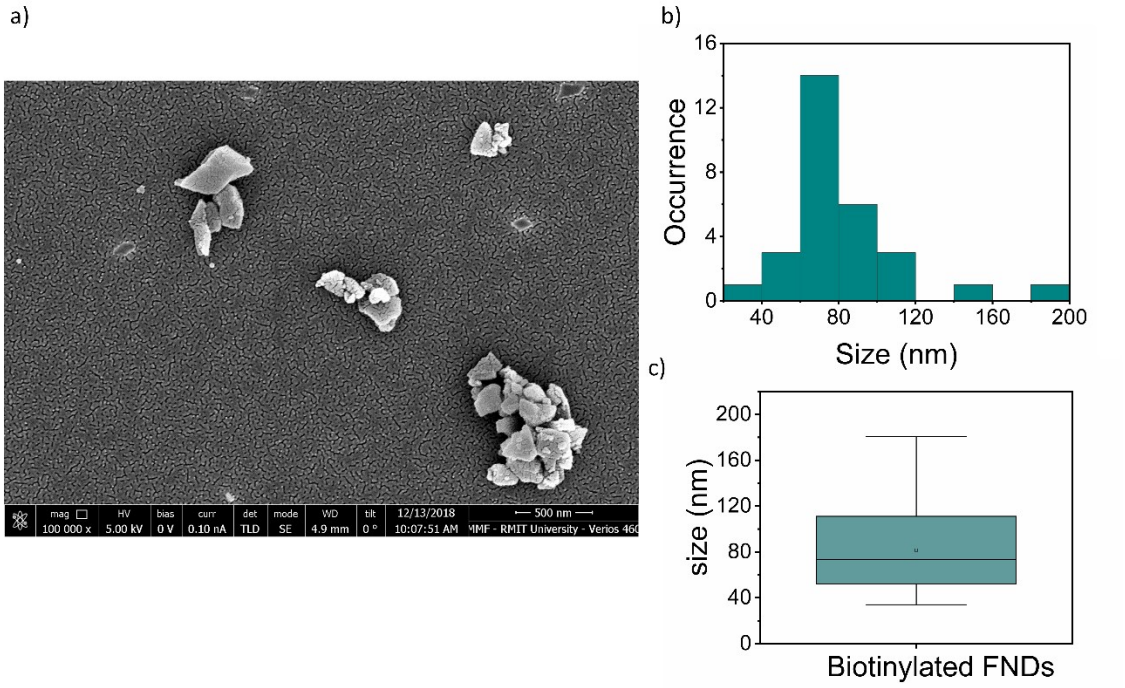

Fig. S10 | Size distribution of biotinylated FNDs. a) SEM image of biotinylated FNDs b) histogram of size distribution occurrence. c) Box chart of size distribution, the outer lines are the minimum and maximum values, the box is the standard deviation. Inside the box: the line is the median, the dot is the mean value.

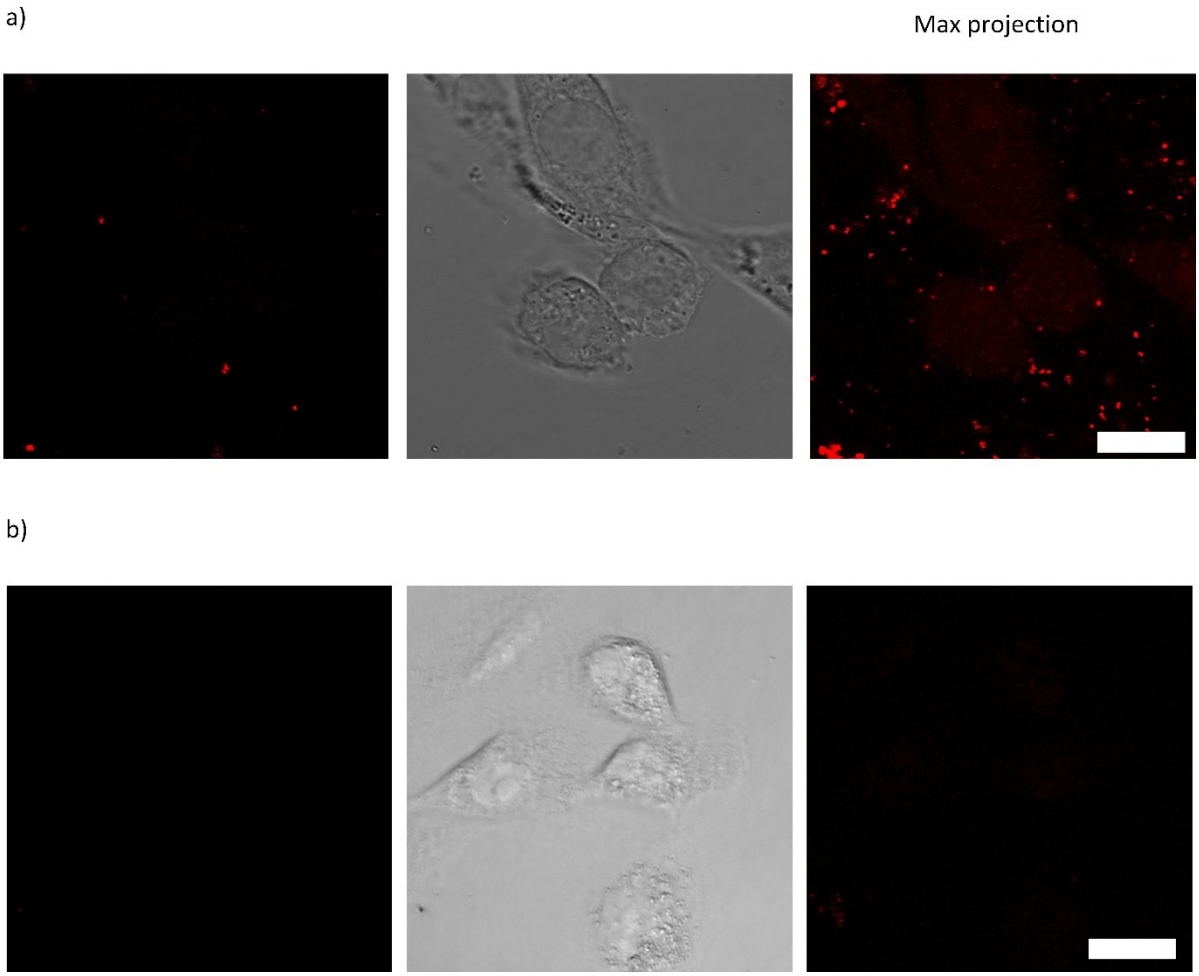

Fig. S11 | Negative controls a) No biotin CD44; 20 nm MNP; 100 nm FND and b) Biotin CD44; no MNP; 100 nm FND. Left: Widefield image of NDs. Centre: brightfield image of MCF10A cells. Right: Maximum intensity projection of z-stack images of NDs.

References

1. Tisler, J. *et al.* Highly Efficient FRET from a Single Nitrogen-Vacancy Center in Nanodiamonds to a Single Organic Molecule. ACS Nano **5(10),** 7893-7898 (2011).